

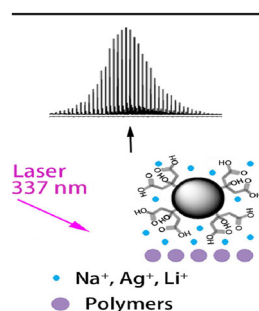
## RESEARCH ARTICLE

# Citric Acid Capped Iron Oxide Nanoparticles as an Effective MALDI Matrix for Polymers

Qiaoli Liang,<sup>1</sup> Jennifer Sherwood,<sup>2</sup> Thomas Macher,<sup>2</sup> Joseph M. Wilson,<sup>2</sup> Yuping Bao,<sup>2</sup> Carolynn J. Cassady<sup>1</sup>

<sup>1</sup>Department of Chemistry, The University of Alabama, Tuscaloosa, AL 35487, USA

<sup>2</sup>Department of Chemical and Biological Engineering, The University of Alabama, Tuscaloosa, AL 35487, USA



**Abstract.** A new matrix-assisted laser desorption ionization (MALDI) mass spectrometry matrix is proposed for molecular mass determination of polymers. This matrix contains an iron oxide nanoparticle (NP) core with citric acid (CA) molecules covalently bound to the surface. With the assistance of additives, the particulate nature of NPs allows the matrix to mix uniformly with polar or nonpolar polymer layers and promotes ionization, which may simplify matrix selection and sample preparation procedures. Several distinctively different polymer classes (polyethyleneglycol (PEG), polywax/polyethylene, perfluoropolyether, and polydimethylsiloxane) are effectively detected by the water or methanol dispersed NPCA matrix with NaCl, NaOH, LiOH, or AgNO<sub>3</sub> as additives. Furthermore, successful quantitative measurements of PEG1000 using polypropylene glycol 1000 as an internal standard are demonstrated.

**Keywords:** Citric acid capped iron oxide nanoparticles, Polymer MALDI matrix

Received: 13 March 2016/Revised: 10 November 2016/Accepted: 14 November 2016/Published Online: 6 December 2016

## Introduction

Matrix-assisted laser desorption ionization (MALDI) mass spectrometry generally utilizes a UV laser (e.g., 337 or 355 nm) to induce ionization of analytes with the assistance of matrices, which absorb and transfer laser energy to the analyte, facilitating analyte desorption and ionization [1]. Although MALDI has been widely used in polymer analysis since its introduction in the 1980s [2–7], the choice of suitable matrices remains complicated. An ideal MALDI matrix (commonly an organic compound) for polymers requires miscibility among sample, matrix, cationizing agent, and solvents. This is sometimes a difficult condition to meet and therefore leads to a large number of matrices and sample preparation procedures [8–10]. For example, a chemometrics approach to optimize MALDI sample preparation for synthetic polymers examined 70 organic matrices [8], and the National Institute of Standards and Technology (NIST) Polymer MALDI MS Method Database currently contains 1250 polymer/matrix combinations,

covering methods reported in scientific literature from 1988 to 2011 [11]. The process of selecting a suitable matrix can be particularly time-consuming for an unknown or newly synthesized polymer. Therefore, development of alternative matrices that can simplify polymer matrix choice and optimize the sample preparation procedure is highly desirable.

In addition to complex matrix and sample preparation choices, quantitative measurement of polymers using MALDI remains challenging. MALDI signal can have limited reproducibility with variances due to laser fluence, voltages, matrix, and sample preparation. Thus, the measured mass distribution by MALDI does not necessarily reflect the true gravimetric (mass) concentration of each oligomer [12, 13], which is particularly problematic for broad molecular mass distribution (MMD) polymers [14]. Nonetheless, a few studies have examined narrow MMD polymer MALDI quantitation with a closely related polymer as an internal standard [15–18]. Among these works [15–18], within a narrow analyte/internal standard gravimetric concentration ratio (~0.5–2), a linear relationship between MS signal and gravimetric concentration is reported. A Taylor expansion mathematical model to determine absolute MMD distribution from measured intensities for narrow disperse polystyrenes has also been proposed [18]. In improving signal reproducibility between replicates, sample preparation

**Electronic supplementary material** The online version of this article (doi:10.1007/s13361-016-1560-4) contains supplementary material, which is available to authorized users.

Correspondence to: Qiaoli Liang; e-mail: liang005@ua.edu

homogeneity is the key. Generally, electrospray deposition is preferred [17, 18] and, when using dried-droplet method, a fast evaporative solvent is used (e.g., tetrahydrofuran) that helps to form homogenous sample/matrix spots [16].

The application of inorganic particles for MALDI analysis dates back to the usage of cobalt nanoparticles by Tanaka in 1988 at the original development of MALDI [6]; however, organic matrices quickly gained popularity [19], and applications using inorganic particle matrices remain limited [20–22]. In recent years, development of nanoparticles (NPs) and nanostructures has resulted in renewed research interests in inorganic particle matrices. A variety of nanomaterials have been applied as MALDI matrices, such as gold [23], silver [24–26], platinum [27, 28], cadmium sulfide [29], silicon [30], titanium oxide [31, 32], and iron oxide [33]. Most existing NP matrix applications to date have focused on peptides, proteins, or small molecule detections, taking advantage of the clean spectral background in the low mass region. Applications of NP matrices for synthetic polymer analysis are limited to a few classes in the <7000  $m/z$  region [34]; for example, porous-silicon for polyesters and polymethyl methacrylate (PMMA) [35, 36], ZnO for polyethylene glycol (PEG), polystyrene (PS), and PMMA [34], graphene for polypropylene glycol (PPG), PS, and PMMA [37], Au@SiO<sub>2</sub> NPs for PEG [38], and halloysite nanoclay for polyester and degradation products [39]. In part, this limited application of NP matrices in polymer analysis is because NP matrices have been less efficient in desorption/ionization of high molecular mass compounds [40], while polymers are often of medium to high molecular mass.

Previously, we have reported glycan characterization with glutathione capped iron oxide nanoparticles as the MALDI matrix [41]. In this study, we will demonstrate for the first time the effectiveness of a citric acid capped iron oxide NP matrix (NPCA) for several distinctively different polymers: PEG, polywax/polyethylene (PE), perfluoropolyether (PFPE), and polydimethylsiloxane (PDMS). Successful quantitative MALDI performance of this new matrix is also demonstrated for PEG.

## Experimental

### Materials

For nanoparticle synthesis, the following chemicals were purchased: ferric ammonium citrate (C<sub>6</sub>H<sub>8</sub>O<sub>7</sub>·xFe·yNH<sub>3</sub>; USB Corporation, Cleveland, OH, USA), hydrazine monohydrate (98%; Alfa Assar, Ward Hill, MA, USA), citric acid anhydrous (99.5%; Acros Organics, Morris Plains, NJ, USA), methanol ACS (99.8%; Alfa Aesar), glutathione (97%, reduced; Alfa Aesar), and thioglycerol (98%; Sigma-Aldrich).

Chemicals for polymer analysis by mass spectrometry include: PEG400, PEG1000, and PPG1000 (Sigma-Aldrich, St. Louis, MO, USA), polywax 1000 (Restek, Bellefonte, PA, USA), PE2000 (Sigma-Aldrich), PFPE Krytox 143AC

(DuPont, Wilmington, DE, USA), silicone oil (Alfa Aesar), PDMS (Scientific Polymer Products, Ontario, NY, USA) 25 and 80 kDa; 2,5-dihydroxybenzoic acid (DHB) was obtained from Bruker Daltonics (Billerica, MA, USA); dithranol (98.5%), trichlorobenzene (anhydrous, 99%), and chloroform (99.9%) were purchased from Sigma-Aldrich. All the other reagents, solvents, and salts were obtained from VWR International (Radnor, PA, USA).

### Synthesis of Iron Oxide NPs

The nanoparticles with citric acid, thioglycerol, and glutathione capping were prepared as follows: ferrous ammonium citrate (20 mg) was mixed with a binary solvent mixture (water, 5 mL; hydrazine, 3 mL) at 100 °C for 1 h. After mixing for 10 min, a capping molecule (citric acid, 26 mg, or thioglycerol 12 μL, or glutathione 41 mg) was added to the solution. After a 1-h reaction, black precipitates of NPs were collected by centrifugation, washed with DI water, and then redispersed into water (0.5 mg/mL) as a MALDI matrix. During the synthesis, hydrazine present in solvent mixture functioned as a reducing agent. The morphology and size of the iron oxide NPs were studied using a Hitachi (Tokyo, Japan) 7860 transmission electron microscope (TEM), and UV/visible spectra were taken in the liquid phase as dispersions on a Shimadzu (Kyoto, Japan) UV-vis spectrophotometer (UV-1700 series).

### Sample Preparation

Polymer samples were prepared as follows: PEG400 1% in water, polywax 1000, and PE2000 5 mg/mL in trichlorobenzene (TCB), PFPE Krytox 143AC 2 μL in 25 μL perfluorohexane, PDMS 25 and 80 kDa, and silicone oil at 6 mg/mL in chloroform. To dissolve polywax and PE in TCB, the glass sample vial was heated on a hotplate at low heat; the dissolved solution turned cloudy after it had cooled down to room temperature prior to spotting onto target.

The matrix conditions include: DHB (5 mg/mL, 50/50 ACN/H<sub>2</sub>O, 0.1% trifluoroacetic acid, TFA), dithranol (10 mg/mL, THF), NPCA-NaCl (0.5 mg/mL NPCA water solution mixed with 300 mM NaCl in water at 9:1 v/v ratio), NPCA-NaOH (0.5 mg/mL NPCA water solution mixed with 300 mM NaOH in water at 9:1 v/v ratio), NPCA-NaOH-LiOH (0.5 mg/mL NPCA-NaOH solution mixed with 300 mM LiOH in water at 9:1 v/v ratio), AgNO<sub>3</sub> (saturated in methanol). A stainless steel target was utilized for sample spotting. PEG and PDMS were spotted on target in a layered dried-droplet method, 1 μL polymer, 0.5 μL of 20 mM NaCl in water, and then 1 μL of DHB or dithranol matrix; or 1 μL polymer followed by 0.5 μL NPCA-NaCl or NPCA-NaOH. Experiments of polywax/PE were prepared by spotting 1 μL AgNO<sub>3</sub> followed by 1 μL of polymer; or 0.5 μL NPCA-NaOH followed by 0.5 μL of AgNO<sub>3</sub> and then 1 μL polymer. Experiments of PFPE were prepared by spotting 1 μL polymer followed by 0.5 μL NPCA-NaOH-LiOH.

For quantitative experiments, 10, 15, 20, 30, or 50 μL of 2 mg/mL PEG1000 in methanol was mixed with 5 μL of 10 mg/

mL PPG1000 (internal standard) in methanol. Additional methanol was added to reach a fixed total volume of 120  $\mu$ L. The 20  $\mu$ L PEG1000 with 5  $\mu$ L PPG1000 sample was used to verify the accuracy of the calibration curve. The NPCA-NaOH matrix in methanol (0.5 mg/mL, 20 mM NaOH) was used for quantitative measurement of PEG1000; 0.5  $\mu$ L NPCA-NaOH in methanol was applied on a stainless steel target and dried. This step was repeated and followed by deposition of 0.5  $\mu$ L of the polymer standards.

### Mass Spectrometry

The MALDI experiments were performed on a Bruker Daltonics (Billerica, MA, USA) Ultraflex I MALDI time-of-flight (TOF) mass spectrometer equipped with a pulsed 337 nm nitrogen laser at 150  $\mu$ J/3-ns, 1-50 Hz. Mass spectra were acquired in reflectron and linear modes, with signal averaging of 500 scans, at 65%–75% of the absolute laser power. For quantitative measurements, the spectra were averaged over 1000 scans with the laser moving in automatic random walk mode, three laser shots at each raster spot. External mass calibration was applied using peptide mixtures in DHB matrix for  $m/z$  100–10,000 and protein mixtures (cytochrome *c* and bovine serum albumin) in sinapinic acid for  $m/z$  10,000–90,000.

For quantitative measurements, automatic peak picking was performed with Bruker software flexAnalysis ver. 3.3. Both  $[M + Na]^+$  and  $[M + K]^+$  ion series were included. Statistical calculations were conducted using Microsoft Excel 2010.

## Results and Discussion

### Synthesis of Citric Acid-capped NP Matrix

The iron oxide NPs were prepared by simply reducing ammonium iron citrate with hydrazine using citric acid as a surface coating. Figure 1a shows the TEM image of NPCA nanoparticles from a typical reaction. The nanoparticles are spherical with an average core size of about 5 nm. The citrate surface coatings are negatively charged at neutral pH in water, where

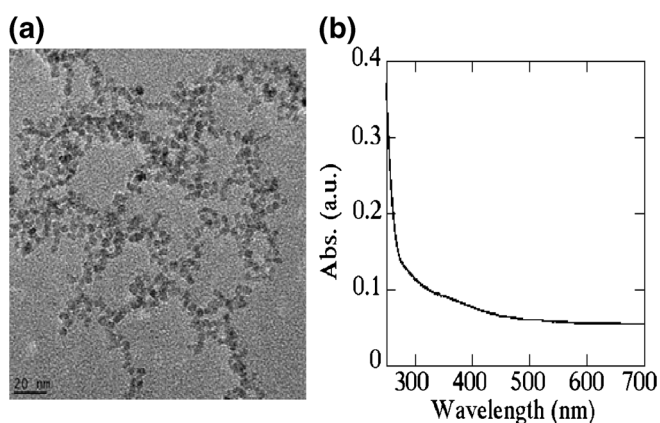


Figure 1. NPCA nanoparticles: (a) TEM image, and (b) UV-vis spectrum

the electrostatic repulsion makes the NPs well dispersed in water. The UV/visible spectrum of the NP water solution (Figure 1b) shows the broad absorption of these NPs below 450 nm, and strong absorption in UV range. The strong absorption in the UV range enables the iron oxide NPs to serve as efficient MALDI matrices to absorb and transfer laser energy.

### NPCA MALDI MS of PEG400

As a commonly studied polymer by MALDI, organic matrices such as DHB work well with PEG [19]. The disadvantage of using organic matrices is that matrix-related ions interfere with the detection of low molecular mass compounds [34]. Similar to other NP matrices such as ZnO [34], graphene [37], halloysite nano-clay [39], and glutathione capped iron oxide nanoparticles [41], NPCA provides a clean spectral background for low molecular mass polymers. This is because NPs are heavy and surface bound during analyte desorption, which eliminates matrix signal from the mass spectra. Additionally, any small molecule impurities that could arise from the NP synthesis are easily removed by the precipitation and washing steps [41].

Figure 2 and insert demonstrate spectra comparison of PEG400 acquired with NPCA, dithranol, or DHB matrix with NaCl as additive. NPCA shows the cleanest spectra in the low mass region, whereas the dithranol spectrum shows the most matrix background. Although the organic matrix background peaks are generally below  $m/z$  300 and do not interfere substantially with the PEG400 spectra, spectra of even lower molecular mass polymers (e.g., PEG 300) could be affected more. For NPCA, DHB, and dithranol matrices, the  $[H(C_2H_4O)_nOH + Na]^+$  ion series are dominant; minor series as indicated in Figure 2 insert include  $[H(C_2H_4O)_nOH + K]^+$  ( $m/z$  409.4,  $n = 8$ ),  $[H(C_2H_4O)_nOH + Na - H_2O]^+$  ( $m/z$  419.4,  $n = 9$ ),  $[CH_3(C_2H_4O)_nOH + Na]^+$  ( $m/z$  407.4,  $n = 8$ ), and  $[CH_3(C_2H_4O)_nOCH_3 + Na]^+$  ( $m/z$  421.4,  $n = 8$ ). Among these minor series, the water loss series is most prominent for DHB matrix, and ion series with extra terminal methyl groups may originate from impurities in the polymer sample. An extra minor ion series of  $[H(C_2H_4O)_nOH + 2Na - H]^+$  ( $m/z$  415.4,  $n = 8$ ) was observed for NPCA only. The observation of disodium ions suggests efficient interaction of  $Na^+$  with the polymer. Disodium ions were also observed for glycans in the presence of a glutathione capped iron oxide NP matrix [41]. The number average molecular mass ( $M_n$ ) calculated by  $[H(C_2H_4O)_nOH + Na]^+$  ion series is 410, 408, and 442 Da for the spectra of NPCA, DHB, and dithranol respectively (compared with  $M_n = 380$ –420 manufacturer value).

### NPCA MALDI MS of Polywax 1000 and PE2000

Hydrocarbons such as polywax or polyethylenes have been difficult to ionize by mass spectrometry because of their chemical inertness [42]. The traditional ionization method of field desorption mass spectrometry (FD/MS) provides intact molecular ions of <3600 Da [43, 44], whereas ionization of higher masses is difficult. Furthermore, FD/MS

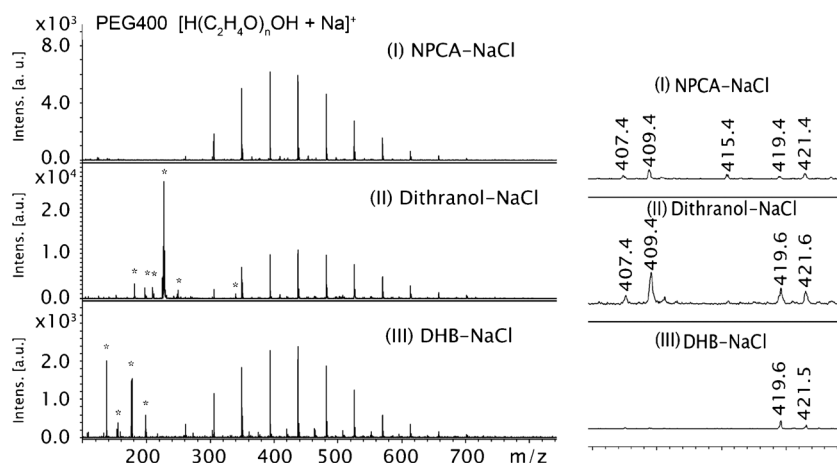


**Figure 2.** MALDI/TOF mass spectra of PEG400 acquired using the (I) NPCA, (II) dithranol, or (III) DHB matrix with NaCl as additive. Insert shows the minor ion series; \* indicates ions from the matrix background

instruments have limited utility and are becoming increasingly difficult to find. More recently, MALDI has been applied to ionize alkanes or polyethylenes <5000 Da using  $\text{AgNO}_3$  as a cation source and a matrix (UV absorptive) [45, 46]. Addition of other media (e.g., organic matrices [45], transition metal powders [22, 45, 47], and silica coated plates or chromatography paper [46]) have been explored for ionization enhancement or fragmentation reduction. Metal powders, silica, and even  $\text{AgNO}_3$  itself are UV absorptive and may serve as a matrix or co-matrix for laser absorption/transfer. Note that some authors refer to ionization assisted with these inorganic materials as laser desorption ionization (LDI) rather than MALDI. In addition, covalent cationization and sample temperature elevation have been investigated to enhance polyethylene MALDI ionization efficiency [48].

Figure 3a and insert compare the polywax spectra taken with  $\text{AgNO}_3$  and NPCA-NaOH/ $\text{AgNO}_3$ . With only  $\text{AgNO}_3$ , mainly  $[\text{H}(\text{C}_2\text{H}_4)_n\text{H} + \text{Ag}]^+$  and silver cluster ions were observed. The NPCA-NaOH/ $\text{AgNO}_3$  combination reduced silver cluster formation and improved spectral resolution but did not introduce new ion series. The improved resolution allowed detailed interpretation of the observed ion series. In addition to the primary ion series  $[\text{H}(\text{C}_2\text{H}_4)_n\text{H} + \text{Ag}]^+$ , other minor fragmentation series include  $[\text{H}(\text{C}_2\text{H}_4)_n\text{H} + \text{Ag}]^+$  ions with 2, 4, and 6H loss (e.g.,  $m/z$  864.0, 862.0, and 860.0 compared with 866.0,  $[\text{H}(\text{C}_2\text{H}_4)_{27}\text{H} + \text{Ag}]^+$ ), and ions with a loss of a  $\text{CH}_2$  from the  $[\text{H}(\text{C}_2\text{H}_4)_n\text{H} + \text{Ag}]^+$  ions without or with further 2, 4, and 6H loss (e.g.,  $m/z$  845.9, 848.0, 850.0, and 852.1 are 14 Da less compared with  $m/z$  860.0, 862.0, 864.0, and 866.0). These dehydrogenation or dealkylation fragment ion series are commonly observed during transition metal interactions with alkanes under laser desorption [22, 45, 47]. Mn calculated with  $[\text{H}(\text{C}_2\text{H}_4)_n\text{H} + \text{Ag}]^+$  ion series for  $\text{AgNO}_3$  and NPCA-NaOH/ $\text{AgNO}_3$  matrix are similar, 981 Da and 974 Da, respectively.

(Compared with manufacturer value C44–C100,  $m/z$  725.6 ~1510.5, GC-MS).

Figure 3b and insert compare the PE2000 spectra acquired with  $\text{AgNO}_3$  and NPCA-NaOH/ $\text{AgNO}_3$ . At the same number of scans (NS = 500), NPCA-NaOH/ $\text{AgNO}_3$  improved signal intensity for PE2000. In addition to the primary ion series  $[\text{H}(\text{C}_2\text{H}_4)_n\text{H} + \text{Ag}]^+$  (e.g.,  $m/z$  1791.0, 1819.1), a minor fragmentation series of  $[\text{H}(\text{C}_2\text{H}_4)_n\text{H} + \text{Ag} - 2\text{H}]^+$  (e.g.,  $m/z$  1789.0, 1817.0) was also observed with NPCA-NaOH/ $\text{AgNO}_3$  matrix. Mn calculated with  $[\text{H}(\text{C}_2\text{H}_4)_n\text{H} + \text{Ag}]^+$  ion series for  $\text{AgNO}_3$  and NPCA-NaOH/ $\text{AgNO}_3$  matrix are similar, 1632 and 1700 Da, respectively, (compared to manufacturer value Mn = 1790, GPC). One effect of NPCA-NaOH may be providing a homogeneous particle-based surface that could affect the  $\text{AgNO}_3$  crystallization process. The addition of NaOH to NPCA matrix is not to provide a source of cation but to improve the nanoparticle dispersion. NPCA without NaOH do not provide distinct resolution or signal enhancement for polywax 1000 or PE2000 samples.

### NPCA MALDI MS of PFPE

Fluorinated polymers such as PFPEs are very hydrophobic and generally only soluble in fluorinated solvents, e.g., perfluorohexane. To improve interaction between fluorinated oligomers and matrix molecules, fluorinated matrices (pentafluorobenzoic acid and pentafluorocinnamic acid) have been employed [49]. Additionally, a salt/polymer/matrix three-layered dried-droplet method, using LiCl and  $\alpha$ -cyano-4-hydroxycinnamic acid (CHCA) was reported from our laboratory [50]. With the LiCl-PFPE-CHCA method, drying of each layer can be time-consuming; furthermore, sweet spots searching and high laser power are often essential for a successful spectrum. In comparison, NPCA-NaOH-LiOH matrix provides a simpler sample preparation approach. The matrix layer spreads homogeneously on top of the fluoropolymer layer, and high quality spectra are readily acquired at medium

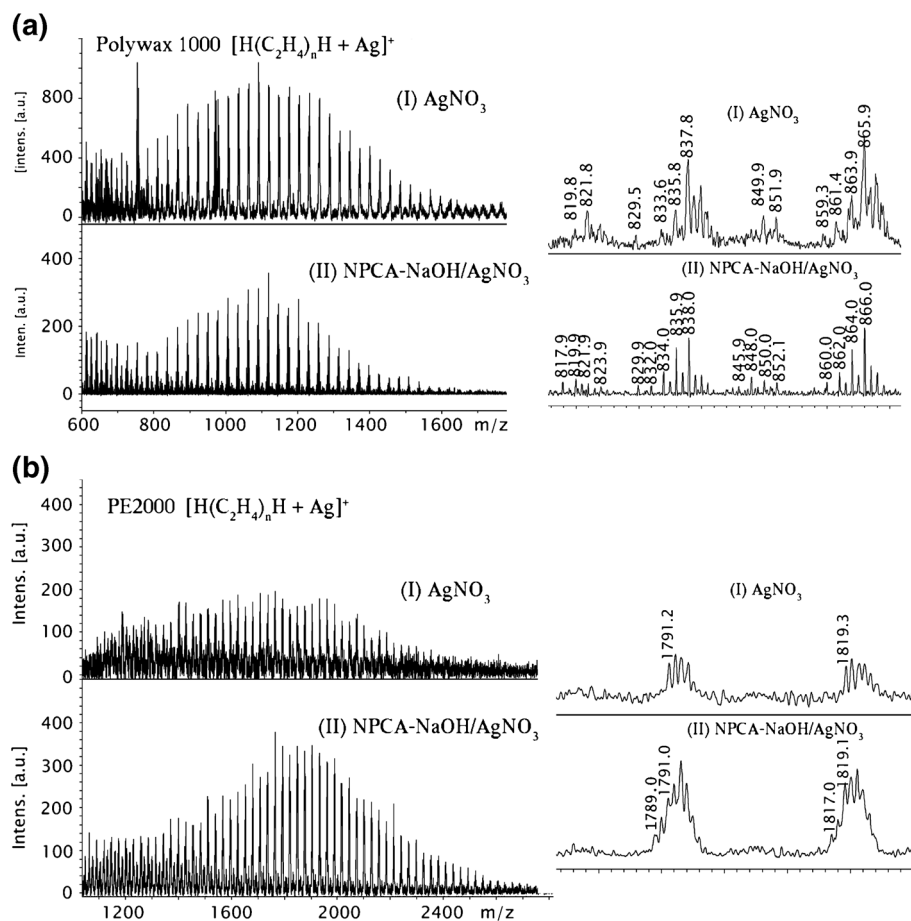


**Figure 3.** MALDI/TOF mass spectra of (a) polywax 1000 and (b) PE2000 acquired with AgNO<sub>3</sub> or NPCA-NaOH/AgNO<sub>3</sub> matrix. Inserts demonstrate [H(CH<sub>2</sub>)<sub>n</sub>H + Ag]<sup>+</sup> as major ions with further 2H, 4H, 6H, or CH<sub>2</sub> loss as minor ions

laser power settings (Figure 4). An intense ion series of [F(C<sub>3</sub>F<sub>6</sub>O)<sub>n</sub>CF<sub>2</sub>CF<sub>3</sub> + Li]<sup>+</sup> was observed for PFPE Krytox 143AC,  $n = 14\sim 50$ ,  $M_n = 5234$ . Other minor ion series correspond to polymer components with extra 1~4 CF<sub>2</sub> end groups (Figure 4 insert). The measured  $M_n$  is lower than the manufacturer value taken by nuclear magnetic resonance (NMR,  $M_n = 5940$  Da). The NMR method calculates the repeating unit by comparing the end group chemical shifts integration with that

of the backbone atoms [51]. Thus, overestimation of the molecular mass could happen if there are multiple end groups present. Since the MALDI spectra indicated the presence of other end groups, the molecular weight measured by NMR could be overestimated.

Lithium(I), Li<sup>+</sup> was chosen for its better ionization efficiency compared with other alkaline ions (Na<sup>+</sup>, K<sup>+</sup>) and simpler isotopic distribution compared with transition

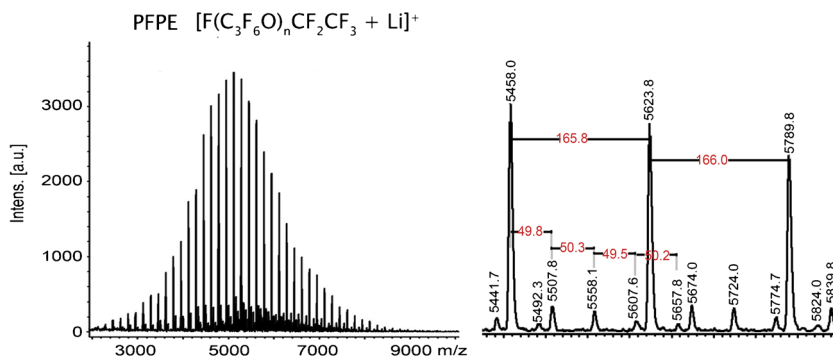


**Figure 4.** MALDI/TOF mass spectra of PFPE Krytox 143AC acquired using the NPCA-NaOH-LiOH matrix. The insert demonstrates the major ion series [F(C<sub>3</sub>F<sub>6</sub>O)<sub>n</sub>CF<sub>2</sub>CF<sub>3</sub> + Li]<sup>+</sup> with a repeating unit of 166 Da, and the minor ion series including 1~4 extra CF<sub>2</sub> (50 Da) groups on the end

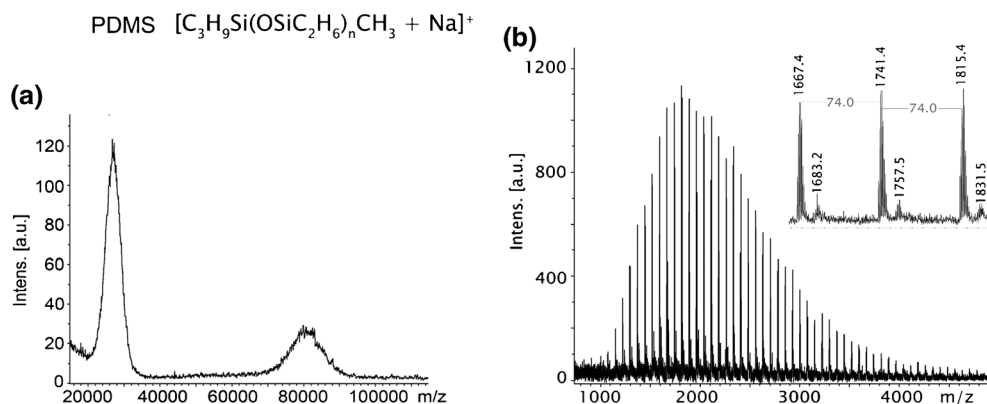


**Figure 5.** MALDI/TOF mass spectra of high and low mass PDMS polymers acquired using the NPCA-NaOH matrix: (a) PDMS 25 KDa and 80 KDa, (b) silicone oil, with insert showing a repeating unit of 74 Da for  $[\text{C}_3\text{H}_9\text{Si}(\text{OSiC}_2\text{H}_6)_n\text{CH}_3 + \text{Na}]^+$  ions

metal  $\text{Ag}^+$  ions [49, 50]. The efficient lithium polymer interaction further improves matrix-polymer homogeneity during sample preparation. As  $\text{Li}^+$  is electrostatically attached onto the negatively charged NP surface,  $\text{Li}^+$ -polymer interaction facilitates NP dispersion on the polymer surface. With added  $\text{Li}^+$ , the NPCA matrix spread to a spot 50% larger in diameter across the Krytox polymer layer compared with that without. Scanning electron microscopy (SEM) images on carbon paper also demonstrate that with  $\text{Li}^+$  the dispersion of NPCA matrix over Krytox polymer is more homogeneous (Supplemental Figure S-1c) compared to without (Supplemental Figure S-1b).

The efficient ionization of polar (PEG) and nonpolar (polywax and PFPE) polymers with NPCA matrix is a result of ideal combination of capping molecules and additives. Citric acid capping provides a negatively charged particle surface that allows facile attachment of metal cations forming electric double layers. (The formation of electric double layer around charged iron oxide nanoparticle surfaces was previously studied by changing counter ions [52], where replacing NP surface monovalent ions with divalent ions caused NP precipitation, while resupplying monovalent ions reversed the process.) This electric double layer interaction facilitates efficient energy transfer from the nanoparticle matrix to polymer molecules

bound to the metal cations ( $\text{Met}^+$ , such as  $\text{Ag}^+$ ,  $\text{Na}^+$ ,  $\text{Li}^+$ ) and thus enhances ionization. With the NPCA matrix, medium laser power is sufficient to produce intense ion signals. This minimizes the sample degradation that can result from higher laser powers. This NPCA- $\text{Met}^+$ -polymer salt bridge type of interaction also greatly improves matrix-polymer miscibility and homogeneity. In this study, aqueous NPCA matrix is evenly dispersed across the hydrophobic polymer surface. This superior homogeneity is a strong point of this particle-based matrix compared with organic matrices for which matrix-polymer segregation often occurs during the matrix crystallization/drying process [53].

### NPCA MALDI MS of HIGH MASS PDMS

High molecular mass polymers pose a challenge for MALDI analysis in general due to the difficulties in desorption and detection [54, 55]. Improvements in sample preparation and detector design have enabled analysis of polystyrene or polyphenylene in the megaDa range [56, 57], but the successes of high mass MALDI experiments have been limited to a few polymer classes [54–57].

High molecular mass analysis with NP matrices has been particularly problematic [40, 58]. The possible cause is that NPs are heavy and surface bound, and thus do not form an abundant

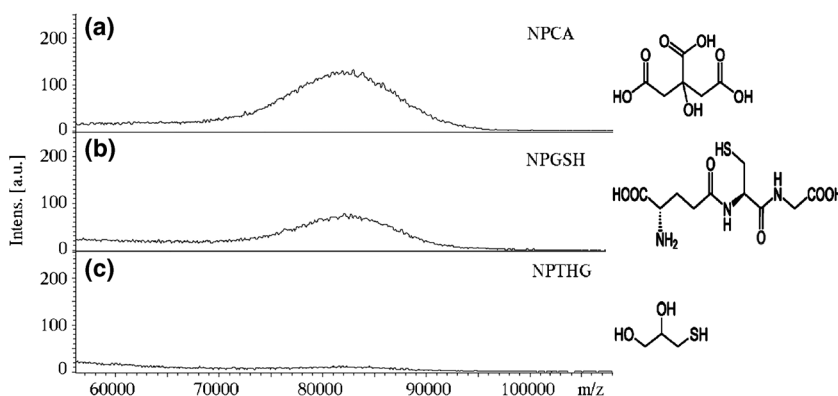


**Figure 6.** MALDI/TOF mass spectra of PDMS 80 kDa acquired using the iron oxide NP matrix (0.5 mg/mL in water, 20 mM NaOH) with different capping molecules: (a) citric acid (NPCA), (b) glutathione (NPGSH), and (c) thioglycerol (NPTHG)

**Table 1.** Preparation of the Standard ( $S_{1-4}$ ) and Verification ( $S_v$ ) Samples of PEG1000 with PPG1000 as internal standard, statistical results of the measured MALDI/TOF MS response

Sample	Wt % PEG/PPG	Vol ( $\mu$ L) 2 mg/mL PEG	Vol ( $\mu$ L) 10 mg/mL PPG	Vol ( $\mu$ L) MeOH	Average $\Sigma m_i I_{i_{peg}} / \Sigma m_i I_{i_{ppg}}$ <sup>a</sup>	Average $\Sigma n_i I_{i_{peg}} / \Sigma n_i I_{i_{ppg}}$ <sup>b</sup>	Average $\Sigma I_{i_{peg}} / \Sigma I_{i_{ppg}}$ <sup>c</sup>	RSD (%)
$S_1$	0.4	10	5	105	0.190	0.249	0.199	5.2
$S_2$	0.6	15	5	100	0.255	0.333	0.269	4.8
$S_3$	1.2	30	5	85	0.682	0.819	0.683	1.6
$S_4$	2.0	50	5	65	1.105	1.452	1.162	1.2
$S_v$	0.8	20	5	95	0.309	0.405	0.326	1.1

<sup>a</sup> $\Sigma m_i I_i$  sum of peak intensity multiplying mass of each oligomer

<sup>b</sup> $\Sigma n_i I_i$  sum of peak intensity multiplying the number of repeating units in each oligomer

<sup>c</sup> $\Sigma I_i$  sum of peak intensity

The averages and relative standard deviation (RSD) values were calculated from three measurements

matrix plume like organic matrices. The lack of matrix molecules/ions in matrix plume results in clean spectral background in low mass spectral region; however, this fails to carry macromolecules into the gas phase. The upper detected mass limits using various NP matrices are generally below 26 kDa for protein samples and 7 kDa for polymers [34, 58]. A HgTe NP matrix was reported to increase the upper mass limit for proteins to 150 kDa [59]. A nanostructure initiator development study involving instant release of the trapped initiator molecules (e.g., 14 kDa poly(3,3,3-trifluoropropylmethylsiloxanes) from silicon pores expanded the protein mass detection range to 30 kDa [60]. It is possible that the success of these approaches lies in more abundant matrix plumes due to the relatively low NP surface melting temperature (HgTe NP, 873K, compared with Au 1337K) or due to release of neutral molecules trapped in nanostructure [60, 61].

Figure 5a demonstrates that the NPCA-NaOH matrix effectively desorbs/ionizes high molecular mass polymers such as 25 and 80 kDa PDMS. As  $\text{Na}^+$  has been reported to assist PDMS ionization in MALDI [62],  $\text{Na}^+$  present in the NPCA matrix is to serve as the cation source to form  $[\text{C}_3\text{H}_9\text{Si}(\text{OSiC}_2\text{H}_6)_n\text{CH}_3 + \text{Na}]^+$ . The broad peak width typical for high mass MALDI [54, 55] precludes repeating unit analysis of polymers. However, the MALDI spectra of a low mass

PDMS (silicone oil) acquired with NPCA-NaOH clearly demonstrated the expected  $[\text{C}_3\text{H}_9\text{Si}(\text{OSiC}_2\text{H}_6)_n\text{CH}_3 + \text{Na}]^+$  ion series with a repeating unit of 74 Da (Figure 5b).

We hypothesize that upon laser ablation, the NPCA matrix releases multiple carbon dioxide ( $\text{CO}_2$ ) molecules from the degradation of capping molecules, which may assist desorption of heavy molecules. In solution, decarboxylation of lauric acid capped iron oxide nanoparticles under 350 nm irradiation has been observed [63]. An iron oxide matrix performance comparison with different capping molecules (e.g., glutathione [41] and thioglycerol) suggests that capping molecules with fewer carboxylic groups result in weaker ion signals for PDMS 80 kDa, as shown in Figure 6. In fact, most organic MALDI matrices have carboxylic groups that could undergo  $\text{CO}_2$  release during laser induced thermal desorption [64]. For instance, a thermal stability study that involved heating matrices at their melting points revealed that sinapinic acid underwent thermal isomerization and  $\text{CO}_2$  loss [65], which may explain why sinapinic acid is an effective matrix for large proteins (200 kDa) [66]. To test this hypothesis, future experiments are planned to integrate a UV laser with a diffuse reflectance infrared Fourier transform spectroscopy-mass spectrometer (DRIFTS-MS). This set-up will allow us to monitor the  $\text{CO}_2$

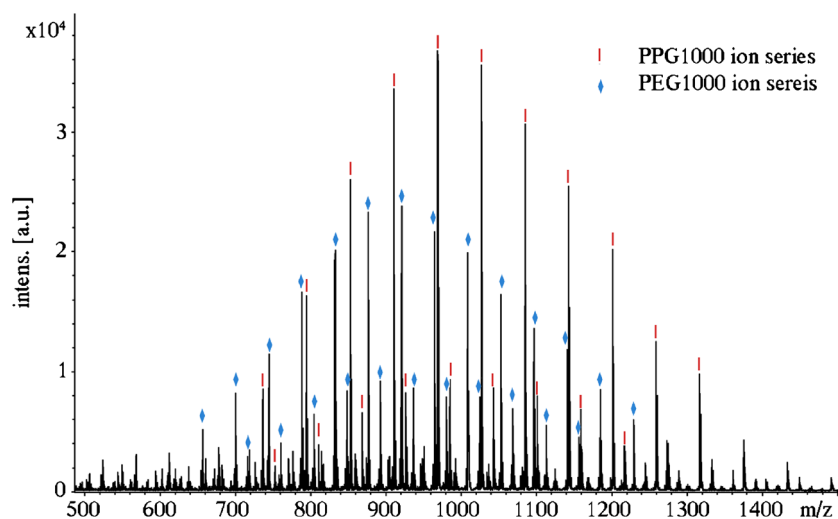


**Figure 7.** MALDI/TOF mass spectra of standard  $S_3$  showing the  $[\text{M} + \text{Na}]^+$  and  $[\text{M} + \text{K}]^+$  ion series of PPG1000 (red bar, internal standard), and PEG1000 (blue diamond, sample)

release in situ and the nanoparticle surface ligand changes under laser ablation.

With the four polymer types studied, the measured molecular mass distribution are comparable with manufacturer values except for PDMS, where the measured masses (25 and 80 kDa) are 16%–25% higher than the manufacturer values [21 and 60 kDa, obtained by gel permeation chromatography (GPC) and light scattering (LS)]. As shown in the Supplemental Figure S-2, the MALDI measured results are relatively reproducible in a different solvent (toluene) at high or low concentration. The low mass PDMS spectra (Figure 5b) demonstrated accurate masses corresponding to the  $[C_3H_9Si(OSiC_2H_6)_nCH_3 + Na]^+$  ions, suggesting the MALDI ionization with NPCA did not introduce new ion types. Thus, mass discrepancy observed may be related to uncertainties in other measurement methods. For instance, the accuracy of GPC results depends upon the use of calibration standards possessing the same or similar structures as the polymer of interest, whereas LS accuracy is affected by molecule shape assumptions and data fitting [67].

### Quantitative Analysis of PEG1000

PEG1000 with PPG1000 as an internal standard was used as a model system to assess the performance of the NPCA matrix for MALDI quantitative measurements. Table 1 summarizes calibration and verification standards preparation and the MS signal response ratio between PEG1000 and PPG1000. Polymers and NPCA matrix were prepared in the volatile solvent methanol instead of water to improve matrix and sample application homogeneity. The MALDI signal reproducibility was best using a 3-layer dried-droplet method, NPCA–NPCA–polymer.

Repeating the NPCA matrix application improves signal reproducibility by creating a more homogeneously distributed NP layer. In addition, the required laser power attenuation was 10% lower with the NPCA application repeated. Lower laser input leads to less sample spot degradation and may also contribute to better reproducibility.

In the literature, several parameters have been used to quantify mass spectrometry responses, including the sum of peak area,  $\Sigma I_{i,area}$  [17]; the sum of peak intensity multiplying the number of repeating units in each oligomer,  $\Sigma n_i I_i$  [16]; and the sum of peak intensity multiplying mass of each oligomer  $\Sigma m_i I_i$  [18, 68]. Linear response has been observed using all three parameters within a narrow sample/internal standard gravimetric ratio range [16–18, 68]. However, with  $\Sigma I_{i,area}$  calculation molar mass difference between internal standard and sample has been shown to incur significant errors in quantification using the standard addition method [17]. Mass-related bias was also observed using  $\Sigma m_i I_i$  when internal standard and sample differ in molecular mass; to counter this problem, a Taylor's expansion method for signal-axis intensity calibration routine was proposed [18]. To minimize mass related quantitative bias, in the current study we simply chose an internal standard of close molecular mass but slightly different repeating groups compared with the sample polymer. The strong intensity  $[M + Na]^+$  and weak intensity  $[M + K]^+$  ion series were both computed into the sum of ion signals. Although close in

mass, Figure 7 demonstrates that PEG1000 and PPG1000 ion series are generally not overlapped.

The PEG1000 versus PPG1000 mass spectrometry response

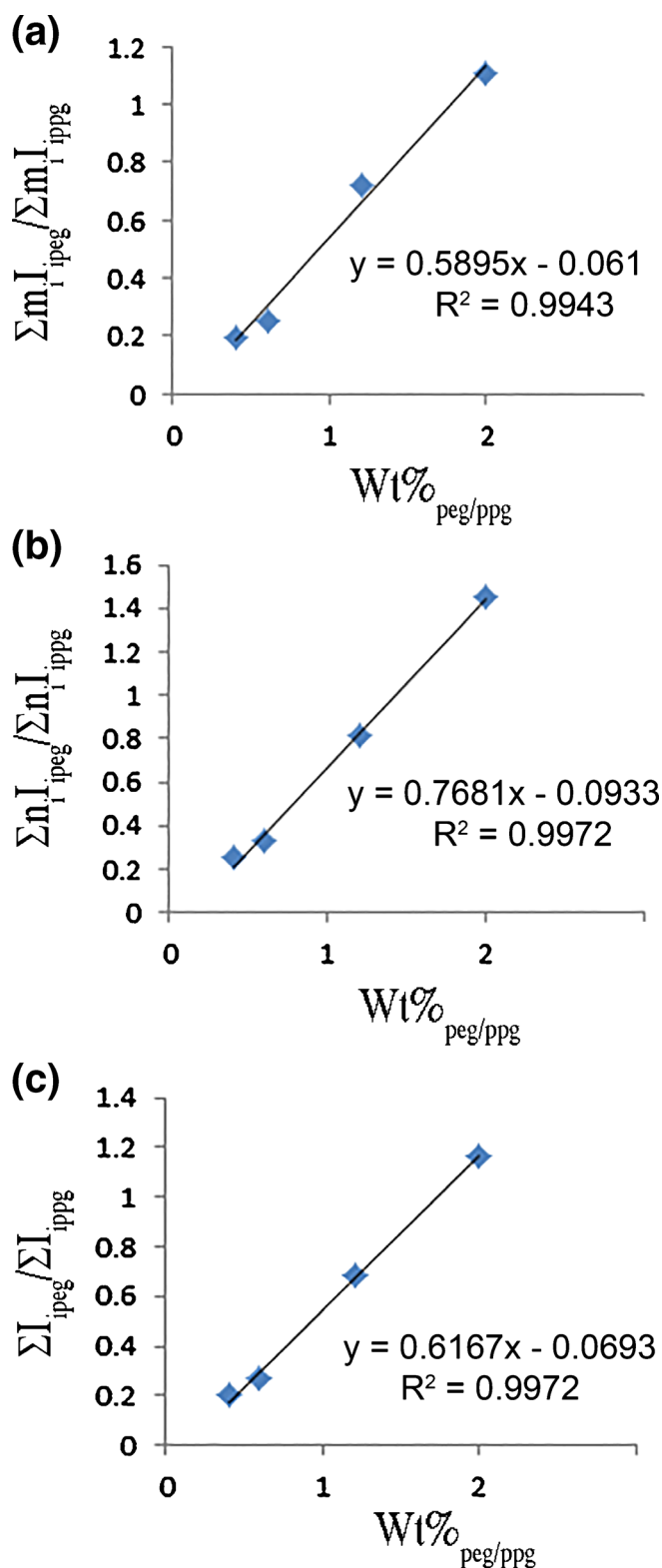


Figure 8. Plots of MALDI/TOF MS average signal of (a)  $\Sigma m_{i,ipeg} / \Sigma m_{i,ippg}$ , (b)  $\Sigma n_{i,ipeg} / \Sigma n_{i,ippg}$ , and (c)  $\Sigma I_{i,ipeg} / \Sigma I_{i,ippg}$  versus gravimetric percentage of PEG1000 to PPG1000, Wt%<sub>peg/ppg</sub>



ratios including  $\Sigma m_i I_{i\text{peg}}/\Sigma m_i I_{i\text{ppg}}$ ,  $\Sigma n_i I_{i\text{peg}}/\Sigma n_i I_{i\text{ppg}}$ , and  $\Sigma I_{i\text{peg}}/\Sigma I_{i\text{ppg}}$  ( $\Sigma I_i$ , sum of peak intensity) are averaged over three replicates and plotted against the gravimetric ratio  $\text{Wt}\%_{\text{peg/ppg}}$  (Table 1 and Figure 8). All plots demonstrate comparable linear relationships and low relative standard deviations ( $<5.2\%$ ), with the  $\Sigma m_i I_{i\text{peg}}/\Sigma m_i I_{i\text{ppg}}$  plot (Figure 8a) having slightly decreased linearity. The calculated verification sample concentrations are also comparable among  $\Sigma n_i I_i$ ,  $\Sigma I_i$ , and  $\Sigma m_i I_i$ , with the calculated PEG/PPG molar ratio as 0.65, 0.64, and 0.63 respectively ( $\sim 20\%$  error compared with the actual ratio of 0.8). Given the 20% error, this quantitative method still has room for improvement. However, quantitative polymer MALDI remains a challenging field in general, and factors affecting accuracy are not completely understood or controlled yet. For example, DHB matrix with PEG samples reported an error range of 1.2% to 705.5% with different MMD PEG internal standard during standard addition [17]; in another report, dithranol matrix with PEG samples [16], only linearity of the relative signal response was demonstrated without an error report.

## Conclusions

A citric acid capped iron oxide nanoparticle matrix is very promising for polymer analysis by MALDI, with clean background for low mass PEG detection and effective detection of polywax/PE, PFPE, and high mass PDMS polymers. The superb matrix-polymer miscibility and ionization efficiency for polymers of different hydrophobicity suggest that the NPCA matrix may function for other polymer classes, and thus simplify the matrix selection and sample preparation process. The linear calibration curve of PEG1000 using PPG1000 as an internal standard demonstrates the NPCA/sample homogeneity and the facile application of this matrix in quantitative MALDI. The use of NPCA for the analysis of other polymer or copolymer samples will be investigated in future work to assess the full utility of this matrix.

## Acknowledgements

The authors gratefully acknowledge financial support from National Science Foundation DMR-0907204 and DMR-1149931 grants, and from a College Academy of Research, Scholarship, and Creative Activity (CARSCA) grant administered through The University of Alabama's College of Arts and Sciences. Y.B. also thanks The University of Alabama Department of Biological Sciences for the use of scanning electron microscope.

## References

- Zenobi, R., Knochenmuss, R.: Ion formation in MALDI mass spectrometry. *Mass Spectrom. Rev.* **17**, 337–366 (1998)
- Li, L.: MALDI mass spectrometry for synthetic polymer analysis. Wiley, Hoboken (2010)
- Hanton, S.: Mass spectrometry of polymers and polymer surfaces. *Chem. Rev.* **101**, 527–570 (2001)
- Gruending, T., Weidner, S., Falkenhagen, J., Bamer-Kowollik, C.: Mass spectrometry in polymer chemistry: a state-of-the-art up-date. *Polym. Chem.* **1**, 599–617 (2010)
- Mautjana, N.A., Pasch, H.: Matrix-assisted laser desorption/ionization mass spectrometry of synthetic polymers. *Macromol. Symp.* **313**, 157–161 (2012)
- Tanaka, K., Waki, H., Ido, Y., Akita, S., Yoshida, Y., Yoshida, T., Matsuo, T.: Protein and polymer analyses up to  $m/z$  100,000 by laser ionization time-of-flight mass spectrometry. *Rapid Commun. Mass Spectrom.* **2**, 151–153 (1988)
- Montaudo, G., Samperi, F., Montaudo, M.S.: Characterization of synthetic polymers by MALDI-MS. *Prog. Polym. Sci.* **31**, 277–357 (2006)
- Brandt, H., Ehmann, T., Otto, M.: Toward prediction: using chemometrics for the optimization of sample preparation in MALDI-TOF MS of synthetic polymers. *Anal. Chem.* **82**, 8169–8175 (2010)
- Hoteling, A.J., Erb, W.J., Tyson, R.J., Owens, K.G.: Exploring the importance of the relative solubility of matrix and analyte in MALDI sample preparation using HPLC. *Anal. Chem.* **76**, 5157–5164 (2004)
- Marie, A., Fournier, F., Tabet, J.: Characterization of synthetic polymers by MALDI-TOF/MS: investigation into new methods of sample target preparation and consequence on mass spectrum finger print. *Anal. Chem.* **72**, 5106–5114 (2000)
- Synthetic polymer MALDI recipes search form. Available at: <http://maldi.nist.gov>. Accessed March (2016)
- Guttman, C.M., Wetzel, S.J., Blair, W.R., Fanconi, B.M., Girard, J.E., Goldschmidt, R.J., Wallace, W.E., VanderHart, D.L.: NIST-sponsored interlaboratory comparison of polystyrene molecular mass distribution obtained by matrix-assisted laser desorption/ionization time-of-flight mass spectrometry: statistical analysis. *Anal. Chem.* **73**, 1252–1262 (2001)
- Wetzel, S.J., Guttman, C.M., Flynn, K.M., Filliben, J.J.: Significant parameters in the optimization of MALDI-TOF-MS for synthetic polymers. *J. Am. Soc. Mass Spectrom.* **17**, 246–252 (2006)
- Montaudo, G., Montaudo, M.S., Puglisi, C., Samperi, F.: Characterization of polymers by matrix-assisted laser desorption/ionization time-of-flight mass spectrometry: molecular weight estimates in samples of varying polydispersity. *Rapid Commun. Mass Spectrom.* **9**, 453–460 (1995)
- Yan, W., Gardella, J.A., Wood, T.D.: Quantitative analysis of technical polymer mixtures by matrix assisted laser desorption/ionization time of flight mass spectrometry. *J. Am. Soc. Mass Spectrom.* **13**, 914–920 (2002)
- Chen, H., He, M.: Quantitation of synthetic polymers using an internal standard by matrix-assisted laser desorption/ionization time-of-flight mass spectrometry. *J. Am. Soc. Mass Spectrom.* **16**, 100–106 (2005)
- Szyska, R., Hanton, S.D., Henning, D., Owens, K.G.: Development of a combined standard additions/internal standards method to quantify residual PEG in ethoxylated surfactants by MALDI TOFMS. *J. Am. Soc. Mass Spectrom.* **22**, 633–640 (2011)
- Guttman, C.M., Flynn, K.M., Wallace, W.E., Kearsley, A.J.: Quantitative mass spectrometry and polydisperse materials: creation of an absolute molecular mass distribution polymer standard. *Macromolecules* **42**, 1695–1702 (2009)
- Bahr, U., Deppe, A., Karas, M., Hillenkamp, F., Giessmann, U.: Mass spectrometry of synthetic polymers by UV-matrix-assisted laser desorption/ionization. *Anal. Chem.* **64**, 2866–2869 (1992)
- Dale, M.J., Knochenmuss, R., Zenobi, R.: Graphite/liquid mixed matrices for laser desorption/ionization mass spectrometry. *Anal. Chem.* **68**, 3321–3329 (1996)
- Schürenberg, M., Dreisewerd, K., Hillenkamp, F.: Laser desorption/ionization mass spectrometry of peptides and proteins with particle suspension matrices. *Anal. Chem.* **71**, 221–229 (1999)
- Yalcin, T., Wallace, W.E., Guttman, C.M., Li, L.: Metal powder substrate-assisted laser desorption/ionization mass spectrometry for polyethylene analysis. *Anal. Chem.* **74**, 4750–4756 (2002)
- McLean, J.A., Stumpo, K.A., Russell, D.H.: Size-selected (2–10 nm) gold nanoparticles for matrix assisted laser desorption/ionization of peptides. *J. Am. Chem. Soc.* **127**, 5304–5305 (2005)
- Kailasa, S.K., Wu, H.: Surface modified silver selenide nanoparticles as extracting probes to improve peptide/protein detection via nanoparticles-based liquid phase microextraction coupled with MALDI mass spectrometry. *Talanta* **83**, 527–534 (2010)
- Jackson, S.N., Baldwin, K., Muller, L., Womack, V.M., Schultz, J.A., Balaban, C., Woods, A.S.: Imaging of lipids in rat heart by MALDI-MS with silver nanoparticles. *Anal. Bioanal. Chem.* **406**, 1377–1386 (2014)

26. Sherrod, S.D., Diaz, A.J., Russell, W.K., Cremer, P.S., Russell, D.H.: Silver nanoparticles as selective ionization probes for analysis of olefins by mass spectrometry. *Anal. Chem.* **80**, 6796–6799 (2008)
27. Shrivastava, K., Agrawal, K., Wu, H.: Application of platinum nanoparticles as affinity probe and matrix for direct analysis of small biomolecules and microwave digested proteins using matrix-assisted laser desorption/ionization mass spectrometry. *Analyst* **136**, 2852–2857 (2011)
28. Kawasaki, H., Ozawa, T., Hisatomi, H., Arakawa, R.: Platinum vapor deposition surface-assisted laser desorption/ionization for imaging mass spectrometry of small molecules. *Rapid Commun. Mass Spectrom.* **26**, 1849–1858 (2012)
29. Kailasa, S.K., Wu, H.: Semiconductor cadmium sulphide nanoparticles as matrices for peptides and as co-matrices for the analysis of large proteins in matrix-assisted laser desorption/ionization reflectron and linear time-of-flight mass spectrometry. *Rapid Commun. Mass Spectrom.* **25**, 271–280 (2011)
30. Wen, X., Dagan, S., Wysocki, V.H.: Small-molecule analysis with silicon-nanoparticle-assisted laser desorption/ionization mass spectrometry. *Anal. Chem.* **79**, 434–444 (2007)
31. Qiao, L., Bi, H., Busnel, J., Liu, B., Girault, H.H.: In-source photocatalytic reduction of disulfide bonds during laser desorption ionization. *Chem. Commun.* **47**, 6357–6359 (2008)
32. Shen, Q., Dong, W., Yang, M., Li, L., Cheung, H., Zhang, Z.: Lipidomic fingerprint of almonds (*Prunus dulcis* L. cv nonpareil) using TiO<sub>2</sub> nanoparticle based matrix solid-phase dispersion and MALDI-TOF/MS and its potential in geographical origin verification. *J. Agric. Food Chem.* **61**, 7739–7748 (2013)
33. Tseng, M., Obena, R., Lu, Y., Lin, P., Lin, P., Yen, Y., Lin, J., Huang, L., Lu, K., Lai, L., Lin, C., Chen, Y.: Dihydrobenzoic acid modified nanoparticle as a MALDI-TOF MS matrix for soft ionization and structure determination of small molecules with diverse structures. *J. Am. Soc. Mass Spectrom.* **21**, 1930–1939 (2010)
34. Watanabe, T., Kawasaki, H., Yonezawa, T., Arakawa, R.: Surface-assisted laser desorption/ionization mass spectrometry (SALDI-MS) of low molecular weight organic compounds and synthetic polymers using zinc oxide (ZnO) nanoparticles. *J. Mass Spectrom.* **43**, 1063–1071 (2008)
35. Gorman, C.B., Petrie, R.J., Genzer, J.: Effect of substrate geometry on polymer molecular weight and polydispersity during surface-initiated polymerization. *Macromolecules* **41**, 4856–4865 (2008)
36. Arakawa, R., Shimomae, Y., Morikawa, H., Ohara, K., Okuno, S.: Mass spectrometric analysis of low molecular mass polyesters by laser desorption/ionization on porous silicon. *J. Mass Spectrom.* **39**, 961–965 (2004)
37. Lu, M., Lai, Y., Chen, G., Cai, Z.: Laser desorption/ionization on the layer of graphene nanoparticles coupled with mass spectrometry for characterization of polymers. *Chem. Commun.* **47**, 12807–12809 (2011)
38. Zhu, X., Wu, L., Mungra, D.C., Xia, S., Zhu, J.: Au@SiO<sub>2</sub> core-shell nanoparticles for laser desorption/ionization time of flight mass spectrometry. *Analyst* **137**, 2454–2458 (2012)
39. Aminlashgari, N., Hakkarainen, M.: Surface assisted laser desorption ionization-mass spectrometry (SALDI-MS) for analysis of polyester degradation products. *J. Am. Soc. Mass Spectrom.* **23**, 1071–1076 (2012)
40. Arakawa, R., Kawasaki, H.: Functionalized nanoparticles and nanostructured surfaces for surface-assisted laser desorption/ionization mass spectrometry. *Anal. Sci.* **26**, 1229–1240 (2010)
41. Liang, Q., Macher, T., Xu, Y., Bao, Y., Cassidy, C.J.: MALDI MS in-source decay of glycans using a glutathione-capped iron oxide nanoparticle matrix. *Anal. Chem.* **86**, 8496–8503 (2014)
42. Wu, C., Qian, K., Nefliu, M., Cooks, R.G.: Ambient analysis of saturated hydrocarbons using discharge-induced oxidation in desorption electrospray ionization. *J. Am. Soc. Mass Spectrom.* **21**, 261–267 (2010)
43. Lattimer, R., Schulten, H.: Field desorption of hydrocarbon polymers. *Int. J. Mass Spectrom. Ion. Phys.* **52**, 105–116 (1983)
44. Gross, J.H., Weidner, S.M.: Influence of electric field strength and emitter temperature on dehydrogenation and CC cleavage in field desorption mass spectrometry of polyethylene oligomers. *Eur. J. Mass Spectrom.* **6**, 11–17 (2000)
45. Chen, R., Yalcin, T., Wallace, W.E., Guttman, C.M., Li, L.: Laser desorption ionization and MALDI time-of-flight mass spectrometry for low molecular mass polyethylene analysis. *J. Am. Soc. Mass Spectrom.* **12**, 1186–1192 (2001)
46. Lorente, E., Berruoco, C., Herod, A.A., Millan, M., Kandiyoti, R.: The detection of high-mass aliphatics in petroleum by matrix-assisted laser desorption/ionization mass spectrometry. *Rapid Commun. Mass Spectrom.* **26**, 1581–1590 (2012)
47. Mennito, A.S., Qian, K.: Characterization of heavy petroleum saturates by laser desorption silver cationization and Fourier transform ion cyclotron resonance mass spectrometry. *Energy Fuels* **27**, 7348–7353 (2013)
48. Wallace, W.E., Blair, W.R.: Matrix-assisted laser desorption/ionization mass spectrometry of covalently cationized polyethylene as a function of sample temperature. *Int. J. Mass Spectrom.* **263**, 82–87 (2007)
49. Marie, A., Alves, S., Fournier, F., Tabet, J.C.: Fluorinated matrix approach for the characterization of hydrophobic perfluoropolyethers by matrix-assisted laser desorption/ionization time-of-flight MS. *Anal. Chem.* **75**, 1294–1299 (2003)
50. Sun, L., Li, Z., Zhu, H., Alfred, W., Liang, Q., Cassidy, C.J., Howell, J.L., Thrasher, J.S.: Characterization of functionalized and non-functionalized perfluoropolyalkylethers by matrix assisted laser desorption ionization/time of flight MALDI/TOF mass spectrometry. *Proceedings of the 59th Southeastern Regional Meeting of the American Chemical Society, Greenville* (2007)
51. Izunobi, J.U., Higginbotham, C.L.: Polymer molecular weight analysis by <sup>1</sup>H NMR spectroscopy. *J. Chem. Educ.* **88**, 1098–1104 (2011)
52. Xu, Y., Qin, Y., Palchoudhury, S., Bao, Y.: Water-soluble iron oxide nanoparticles with high stability and selective surface functionality. *Langmuir* **27**, 8990–8997 (2011)
53. Weidner, S.M., Falkenhagen, J.: Imaging mass spectrometry for examining localization of polymeric composition in matrix-assisted laser desorption/ionization samples. *Rapid Commun. Mass Spectrom.* **23**, 653–660 (2009)
54. Schriemer, D.C., Li, L.: Detection of high molecular weight narrow polydisperse polymers up to 1.5 million Daltons by MALDI mass spectrometry. *Anal. Chem.* **68**, 2721–2725 (1996)
55. Weidmann, S., Mikutis, G., Barylyuk, K., Zenobi, R.: Mass discrimination in high-mass MALDI-MS. *J. Am. Soc. Mass Spectrom.* **24**, 1396–1404 (2013)
56. Aksenov, A.A., Bier, M.E.: The analysis of polystyrene and polystyrene aggregates into the mega Dalton mass range by cryodetection MALDI TOF MS. *J. Am. Soc. Mass Spectrom.* **19**, 219–230 (2008)
57. Räder, H.J., Nguyen, T., Müllen, K.: MALDI-TOF mass spectrometry of polyphenylene dendrimers up to the megadalton range. Elucidating structural integrity of macromolecules at unrivaled high molecular weights. *Macromolecules* **47**, 1240–1248 (2014)
58. Chiang, C., Chiang, N., Lin, Z., Lan, G., Lin, Y., Chang, H.: Nanomaterial-based surface-assisted laser desorption/ionization mass spectrometry of peptides and proteins. *J. Am. Soc. Mass Spectrom.* **21**, 1204–1207 (2010)
59. Chiang, C., Yang, Z., Lin, Y., Chen, W., Lin, H., Chang, H.: Detection of proteins and protein-ligand complexes using HgTe nanostructure matrices in surface-assisted laser desorption/ionization mass spectrometry. *Anal. Chem.* **82**, 4543–4550 (2010)
60. Northen, T.R., Yanes, O., Northen, M.T., Marrinucci, D., Uritboonthai, W., Apon, J., Golledge, S.L., Nordström, A., Siuzdak, G.: Clathrate nanostructures for mass spectrometry. *Nature* **449**, 1033–1036 (2007)
61. Chen, W., Chiang, C., Lee, C., Chang, H.: Using surface-assisted laser desorption/ionization mass spectrometry to detect proteins and protein-protein complexes. *Anal. Chem.* **84**, 1924–1930 (2012)
62. Liu, X.M., Maziarz, E.P., Heiler, D.J., Grobe, G.L.: Comparative studies of poly (dimethyl siloxanes) using automated GPC-MALDI-TOF MS and online GPC-ESI-TOF MS. *J. Am. Soc. Mass Spectrom.* **14**, 195–202 (2003)
63. Dadashi-Silab, S., Yar, Y., Acar, H.Y., Yagci, Y.: Magnetic iron oxide nanoparticles as long wavelength photoinitiators for free radical polymerization. *Polym. Chem.* **6**, 1918–1922 (2015)
64. Knochenmuss, R.: Ion formation mechanisms in UV-MALDI. *Analyst* **131**, 966–986 (2006)
65. Tarzi, O.I., Nonami, H., Erra-Balsells, R.: The effect of temperature on the stability of compounds used as UV-MALDI-MS matrix: 2, 5-dihydroxybenzoic acid, 2, 4, 6-trihydroxyacetophenone,  $\alpha$ -cyano-4-hydroxycinnamic acid, 3,5-dimethoxy-4-hydroxycinnamic acid, norharmene, and harmene. *J. Mass Spectrom.* **44**, 260–277 (2009)
66. Ludwig, K., Habbach, S., Krieglstein, J., Klumpp, S., König, S.: MALDI-TOF high mass calibration up to 200 kDa using human recombinant 16 kDa protein histidine phosphatase aggregates. *PLoS One* **6**, e23612 (2011)
67. Montaudo, G., Lattimer, R.P.: *Mass Spectrometry of Polymers*. CRC Press, Boca Raton (2002)
68. Walterová, Z., Horský, J.: Quantification in MALDI-TOF mass spectrometry of modified polymers. *Anal. Chim. Acta* **693**, 82–88 (2011)